



On the development of a collaborative robotic system for industrial coating cells

Rafael Arrais^{1,2} · Carlos M. Costa^{1,2} · Paulo Ribeiro¹ · Luís F. Rocha¹ · Manuel Silva^{1,3} · Germano Veiga^{1,2}

Received: 31 August 2020 / Accepted: 24 September 2020 / Published online: 13 October 2020
© Springer-Verlag London Ltd., part of Springer Nature 2020

Abstract

For remaining competitive in the current industrial manufacturing markets, coating companies need to implement flexible production systems for dealing with mass customization and mass production workflows. The introduction of robotic manipulators capable of mimicking with accuracy the motions executed by highly skilled technicians is an important factor in enabling coating companies to cope with high customization. However, there are some limitations associated with the usage of a fully automated system for coating applications, especially when considering customized products of large dimensions and complex geometry. This paper addresses the development of a collaborative coating cell to increase the flexibility and efficiency of coating processes. The robot trajectory is taught with an intuitive programming by demonstration system, in which an icosahedron marker with multicoloured LEDs is attached to the coating tool for tracking its trajectories using a stereoscopic vision system. For avoiding the construction of fixtures and allowing the operator to freely place products within the coating work cell, a modular 3D perception system was developed, relying on principal component analysis for performing the initial point cloud alignment and on the iterative closest point algorithm for 6 DoF pose estimation. Furthermore, to enable safe and intuitive human-robot collaboration, a non-intrusive zone monitoring safety system was employed to track the position of the operator in the cell.

Keywords Collaborative robotics · Safety · Flexible robotics · Smart manufacturing · Industry 4.0

1 Introduction

The ongoing Fourth Industrial Revolution is altering the industrial ecosystem in many different domains. Besides the traditional technological novelties associated with this period in time, such as the emergence of fully interoperable Cyber-Physical System (CPSs) [1–3] and the Internet of Things (IoT) [4–6], that are so often encapsulated under the Industry 4.0 umbrella [7, 8], these ongoing modifications of manufacturing paradigms are also deeply impacting the way companies are interacting with one another and

with customers. Industrial enterprises are changing their internal processes and adapting their production approaches to address the sustainable increase in demand diversity, an emblematic characteristic of the ongoing industrial revolution [9]. This contemporary growth in demand variety directly results in low volumes per order and products with shorter life cycles, two traits that undeniably contrast with the business model and production paradigms entrenched over the last decades in many industrial sectors [10]. Also, while addressing these dilemmas, enterprises have to improve the quality and reliability of produced goods, oversee costs, and manage environmental impacts [11]. In complement, the ageing demographics of the western society is imposing added challenges in engaging, training, and preserving qualified industrial operators, which can be an added shortcoming for industrial sectors requiring skilful personnel for the execution of some particularly demanding tasks [12].

The technological advancements emerging under the Industry 4.0 banner can play a significant role in assisting industrial companies to address the aforementioned

✉ Rafael Arrais
rafael.l.arrais@inesctec.pt

¹ INESC TEC - INESC Technology and Science, Rua Dr. Roberto Frias, 4200-465, Porto, Portugal

² Faculdade de Engenharia da Universidade do Porto, Rua Dr. Roberto Frias, 4200-465, Porto, Portugal

³ Instituto Superior de Engenharia do Porto, Rua Dr. Ant. Bernadino Almeida, 4200-072, Porto, Portugal

challenges. In particular, the introduction of CPSs such as modern robotic systems for the enhancement of productivity, production flexibility, working conditions and ergonomics, and for the automation of non-added value tasks is a major trump being utilized by companies to comply with the illustrated paradigmatic changes in the present-day manufacturing culture [13]. By definition, CPSs are interconnected through IoT platforms not only with Manufacturing Execution System (MES) and Enterprise Resource Planning (ERP) systems but also with existing industrial equipment [14]. This fully interoperable industrial manufacturing environment can also be a decisive factor in enhancing production quality and product traceability, thus positively contributing to the improvement of the produced goods.

As previously referred, some particular industrial sectors are facing more resistance to adapt to the mass customization production paradigm, for a myriad of reasons, which range from adversities of adapting elemental steps in the manufacturing processes to highly customized products, all the way to the complications associated with the supply chain of a wide array of lot-size-one finished goods. In the domain of industrial coating, one of the fundamental activities is the spraying of complex and delicate products, a highly scrupulous process that, due to the accuracy and reliability requirements is traditionally only performed manually, by highly skilled operators with several years of training. The manual nature of the way this manufacturing step is traditionally executed contrasts with the current business requirements associated with production flexibility, as many companies in the sector do not have enough qualified personnel to comply with frequent changes in the process, as the introduction of a customized part requires a time-consuming training phase of the workforce [12].

To improve the flexibility of the process, to cope with a vastly customized demand, and to enhance the efficiency of the coating process with the objective of matching the expected throughput, a previous R&D initiative, the SIIARI project¹, aimed at pushing forward the development of technology for a highly adaptive, intuitive, and non-intrusive robotic programming by demonstration framework for coating applications. This successful R&D initiative originated a programming by demonstration system, 6D MIMIC [15], that allows the transfer of human know-how to industrial robots, thus allowing the automation of coating applications. This pioneering project was demonstrated at Flupol Surface Engineering S.A. (FLUPOL), a Portuguese Small and Medium-sized Enterprise (SME), founded in 1986, focused on the application of coating on the surface of technical parts. FLUPOL's range of application varies from houseware utilities, automotive and aerospace parts,

components for the baking and textile industries, and any general industrial application where advanced coating is required for surface adhesion, dry lubrication or corrosion prevention.

Currently, FLUPOL makes use of the outputs of the SIIARI project on its daily operation, where an industrial manipulator is frequently reprogrammed by skilled operators on how to perform complex and precise coating operations. Due to the facility in transferring human expertise in the form of precise manoeuvres associated with the coating process, the company can rely on an industrial manipulator to perform some operations that, until recently, could only be performed by highly skilled technicians.

Despite the success of the automated solution, the last years have shown that there was still room for improvement, namely in the processing of large and complex parts. These parts were still being coated manually, mostly due to the limited reach of robotic solutions. Namely, with some parts, the robot would need one external axis (a rail track) to be able to coat all the parts, and in other cases (e.g. in parts with internal cavities) it would need a two-axis external positioner to reorient the part for the robot to reach the entire surface. A robotic work cell that could cope with all this variability would be very expensive and would impose severe layout constraints on the shop floor. With the 6D MIMIC automated solution, due to safety limitations, it was impossible to have a human and an industrial robot sharing the same work environment. In the automated process, the operator starts by spraying a prototype object, having the developed teaching solution coupled to the coating gun, transferring by this mean the coating skill to the industrial robot. Then, in a subsequent phase, the robot, isolated in a dedicated and enclosed cell, can perform the same motions on an actual production component. In this production scenario, simultaneous collaboration is not possible, which plays an important limitation for coating complex or large-scale objects.

To address the aforementioned limitations, and to allow the company to successfully coat both large-scale and complex components, the FLEXCoating experiment² was proposed under the H2020 HORSE³ project. Due to restrictions associated with the full automation of the coating operation previously enumerated, and due to the underlying craftiness and refinement of the coating process, which elevates the operator's collective know-how of the process to one of the main assets within this industrial sector, the main premise of the FLEXCoating experiment was to combine the expertise of human operators with the potential for added flexibility and efficiency associated with robotic solutions.

²<http://horse-project.eu/FLEXCoating>

³<http://horse-project.eu/>

¹<https://www.inesctec.pt/en/projects/siari>

In this paper, the FLEXCoating results will be presented in detail. The main scientific contribution of this work was the development of the first collaborative robotic application in the industry of coating, where humans and robots can simultaneously collaborate on coating large and complex components. The development, deployment, and testing took place in a real operational scenario, with real technicians and production equipment. The fully automated work cell was adapted to accommodate the industrial sensors that provided the necessary safety measures and usability upgrades for allowing an effective and safe collaboration between humans and robots.

The remainder of this paper is organized as follows: Section 2 describes related work. In Section 3 a thorough analysis of the manufacturing process of coating in the end-user industrial facilities will be presented, with an emphasis on the conceived collaborative coating operation. Section 4 will provide an overview of the collaborative coating cell system architecture, highlighting its integration with the HORSE framework. Section 5 will detail the set of technological pillars empowering the establishment of the collaborative coating cell. Section 6 will overview the metrics associated with the operational evaluation of the industrial demonstration of the FLEXCoating experiment; Finally, in Section 7, conclusions are outlined and future work topics are discussed.

2 Related work

The last few decades have witnessed a strong movement in the robotics community, both by manufacturers and research entities, towards the development of more flexible robotics equipment. This flexibility is a composition of varied contributions, namely, new and more intuitive programming methods [15, 16], advanced interface systems (Plug‘n’Produce) [17, 18], better sensors [19, 20] and more flexible and agile grippers [21].

The development of new collaborative robotic manipulators, which can work side by side with humans, due to their design and safety characteristics, has opened up new possibilities to improve the flexibility of the manufacturing lines [22, 23]. Tasks that until now were performed only by shop floor operators (due to the complexity of the operations or the cognitive requirements) started to be performed in cooperation between humans and robots [24, 25]. When adopting collaborative robots at the shop floor it is necessary to always pay attention to the peripherals used in these applications, such as the tools used by the robots, the weight and speed of the loads to be moved, in order to validate whether or not it is necessary to introduce safety equipment. It is also necessary to assess the operator’s body areas exposed to risks so that the speed of the collaborative robot

is adjusted accordingly. These are some of the main reasons why the adoption of collaborative robots for a certain industrial application requires a previous careful analysis of the operation and respective environment where it will be installed, so to guarantee that they are the best choice for the problem at hand; otherwise, one can run the risk of its adoption harming the performance of the production system.

Collaborative robots are undoubtedly one of the strongest emblems of Industry 4.0, and play a major role in making production lines more agile. However, they are not the only solution for implementing collaborative robotic systems, and they are often not even the most appropriate ones to adopt [26].

According to the international standards ISO 10218 (part 1 and part 2) [27, 28], and ISO/TS 15066 [29], the solutions to make a robotic system collaborative can be categorized into four distinct types: (i) the Safety Monitored Stop; (ii) the Hand Guiding; (iii) the Speed and Separation Monitoring, and; (iv) the Power and Force Limiting type. Safety mechanisms are in constant evolution, providing new ways of assuring safety conditions for humans and machines such as industrial robots to operate, cooperatively, in the same workspace. Traditionally, in industry, it is common to find safety guards and physical barriers that cordon off robots from people, in an attempt to prevent accidents from fast-moving operations [30]. Typically, if an operator needs to enter the robot workspace the robot would be brought to a full stop. But, there are safety technologies available on the market that allow slowing the robot to a safe speed, making possible the operation of the robot and the human operator in the same workspace [31]. One example of this kind of technology is the PILZ SafetyEYE sensor, a safety camera system for 3D zone monitoring [32]. More precisely, this sensor is based on three greyscale cameras, mounted above the production areas under scrutiny. Through the provided software, it is possible to customize the warning and detection zone along the envelope of the danger zone or work area.

In this regard, it is nowadays possible to verify, and in line with the Industry 4.0 paradigm, an evolution of the industrial robotic cells, shifting from being completely enclosed and isolated from human operators to more collaborative setups [33–35]. In the literature, it is already possible to see this paradigm shift in different application areas and in different industrial sectors [36–38]. Particularly, the use of collaborative robots in the manufacturing industry have a tendency to occupy fundamentally production operations [39, 40], such as assembly tasks [35, 41–44], pick-and-place, and logistics functions [45–47].

Concerning the automated painting and application of coating to parts, it is a task that is currently performed by

robots in several distinct industrial areas [48–50]. However, it is not common to have humans collaborating with robots performing these tasks, due to the need to maintain stringent air quality characteristics inside the painting booth. The traditional approach for automated painting and coating tasks is to have one or more robots enclosed on a cell (booth) performing the operation, while the human operators feed the robots with parts to be coated and remove the finish parts while, in some cases, also performing a visual quality inspection of the part finishing. To the best of the authors' knowledge, the only developed human-robot collaboration (HRC) painting task is for the interior finishing of industrial developments [51].

Given these ideas, this paper presents an innovative industrial collaborative coating cell, enabling the simultaneous coating of a single part by a human operator together with an industrial (non-collaborative) robot.

3 Manufacturing process analysis

This paper addresses the conversion of an existing fully automated coating cell into a one-of-its-kind collaborative coating cell on an end-user production line. This cell targets coating large parts and/or parts with complex geometry through close collaboration between a human operator and a robot, which is an operation that the fully autonomous robot cannot effectively perform, as previously discussed.

The top-level production scenario overview and the particularities of the collaborative coating production step are represented in Figs. 1 and 2, respectively, through diagrams employing the Business Process Model Notation (BPMN) 2.0 [52, 53]. The BPMN is a Business Process Model Language (BPML) that has been extensively used in industry and research to map business processes, clearly and systematically identifying actions, roles, interactions, and data flows [54], allowing an intelligible share of knowledge and information between people of different backgrounds [55]. The application of the BPMN concept to support the execution of manufacturing tasks have been

introduced in [56], through a novel process management system, the Manufacturing Process Management Software (MPMS) [57], that orchestrates the manufacturing tasks across different production resources spread throughout the industrial shop floor. The MPMS will be further detailed in Section 5.1.

The first stage of the process, as seen in Fig. 1, is the reception of material according to the respective production order, followed by an initial inspection to evaluate the state of the received parts and check if they can be accepted. This preliminary validation assesses if the parts fulfil the minimum requirements to be coated. If, for any reason, a given part lot is not accepted, it is sent back to the client without the coating. The stage of inspection is also responsible to check if the respective part requires the degreasing process or not. If not, the part skips the degreasing process and goes directly to the surface preparation phase. If this process is needed, the degreasing process is applied before the surface treatment, which has the objective of preparing the part for the coating process, eliminating the impurities in it. After the coating stage, the parts proceed to the curing stage, followed by the final inspection of the coated parts, evaluating whether they meet all the requirements imposed by the client and are ready to be shipped.

Figure 2 showcases the BPMN diagram focused on the manufacturing steps performed at the collaborative coating cell level. The action sequence starts with loading the part number and the corresponding batch size into the system, where an internal checker verifies if the part reference is known (i.e. if it exists in a relational database). If the part number does not exist, that means that the robot is not capable of coating that kind of part yet, as there is not yet a reference to a robot program on the database to coat that specific type of part. Therefore, in these situations, the next step consists of teaching the robot how to coat it, using the programming by demonstration methodology, 6D MIMIC, which will be discussed in Section 5.4. If the program generated by the programming by demonstration methodology is not approved or some error happens during

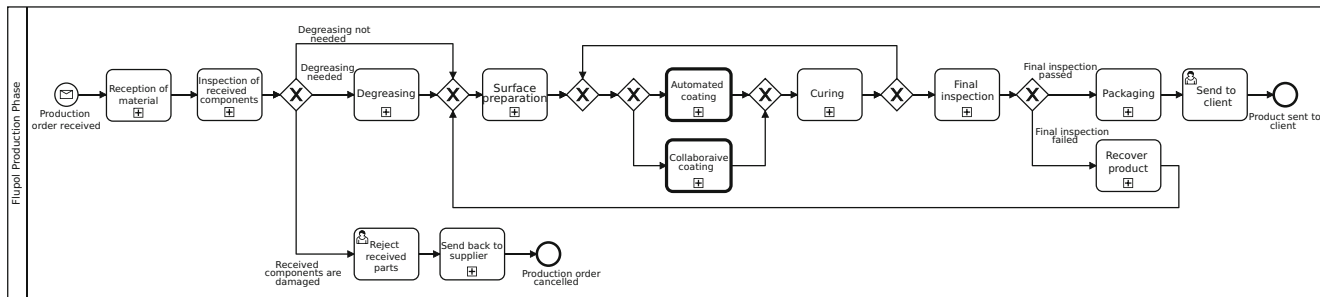


Fig. 1 Manufacturing process analysis of the coating end-user production line represented as a BPMN diagram. Steps with a bold border represent the coating application phase, either collaborative or fully automated

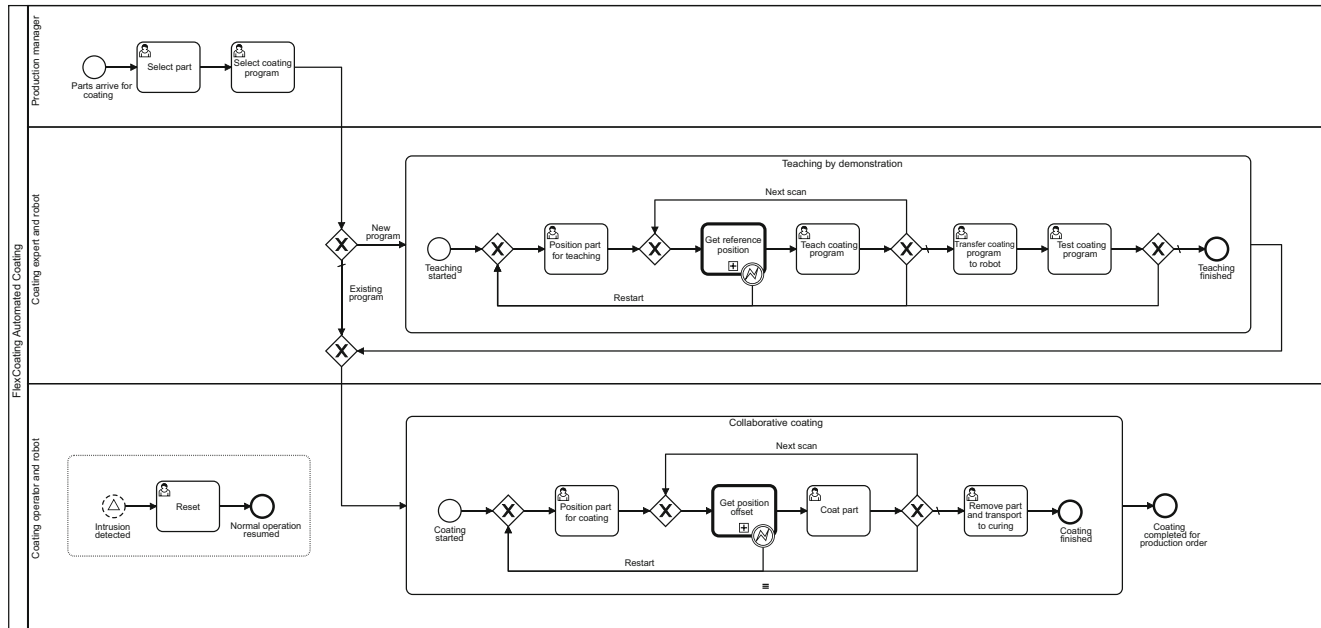


Fig. 2 Manufacturing process analysis of the collaborative coating cell represented as a BPMN diagram. The horizontal lanes represent the three different agents involved in the operation: the production

manager, the team composed by the coating expert and the robot, and the team composed by the coating operator and the robot

the teaching process, this step is repeated until the program is within the desired patterns. Once the program is approved, it is transferred to the robot and it is tested on a prototype part, as to evaluate the performance of the robot. If the coating is applied with success, the program is stored on a file system and referenced in a database, allowing it to be later invoked to coat that kind of part. If the coating expert disapproves the coating applied by the robot, the process of teaching the robot is repeated until it reaches the coating requirements.

Once the coating trajectory has been saved, it can be selected and used on the collaborative coating process. The start of the coating process is triggered by the placement of the part to be coated on the rotating coating table. At the start of the coating process, and every time the coating table is moved, the robot dynamically adjusts its movement trajectory according to the localization of the part, thanks to the developed object localization system, further detailed in Section 5.5. During the collaborative coating operation, when a non-safe situation is detected by the HRC safety system, addressed in Section 5.3, a parallel monitoring process state is triggered, which is responsible to safely halt the coating process until a *reset* command is issued by the operator. Once the collaborative coating is finished, the coated part is removed from the table by the coating operator and the process is finalized.

4 System architecture

The collaborative coating cell conversion was based on the HORSE project system architecture, complementing it with additional software agents and modules. As detailed in [57, 58], the HORSE system architecture was defined considering a software engineering 4+1 framework [59] to address the different perspectives of the system by different actors, and a business information systems design framework [60] to consider and model the interoperability with enterprise information systems and their corresponding notation. Having these frameworks as starting points, the HORSE software architecture was idealized from a top-down perspective, resulting in a level-based approach for organizing functional modules.

On typical enterprise architectures, the HORSE system can be positioned between the production resources (human operators, robotic system, automation equipment, etc.) and traditional manufacturing systems such as MES and ERP modules [61]. As detailed in [62], the HORSE logical software architecture is organized in six different aggregation levels; however, only the first four levels were considered during the design of the collaborative coating cell system architecture.

The first level, level 0, is where the HORSE system modules are contextualized with the enterprise information

systems that support the manufacturing process, such as end-to-end Business Process Management (BPM) systems, MES, and Product Lifecycle Management System (PLMS) [63]. For this work, the enterprise-level modules of the end-user were emulated, as not only their integration was outside the scope of the project, but also the integration effort would directly impact ongoing production and business processes, which was deemed as undesirable. The second level, level 1, introduces the concept of the Global and Local domains, relatable to traditional discrete production representations on the International Electrotechnical Commission (IEC) hierarchy for manufacturing [64]. The HORSE Global domain encompasses higher levels of the production architecture, while the HORSE Local domain directly involves processes running on a shop floor level. Level 2 further decomposes the Global and Local domains into four modules, two for each domain: design and configuration; and execution. For the proposed coating cell conversion, the Global domain design and configuration layer relates to the creation and optimization of the process models encoded using the BPMN, presented in Section 3. Similarly, the HORSE Global domain execution level relates to the utilization of the MPMS to orchestrate the execution of manufacturing operations on the collaborative coating cell, as will be detailed in Section 5.1.

The integration of the FLEXCoating modules with the MPMS was enabled by the development of connectivity agents between these components and the HORSE Cyber-Physical Middleware, as will be discussed in Section 5.2. Several different components were integrated into the HORSE system architecture, thanks to the interconnectivity with the HORSE Cyber-Physical Middleware, namely: (i)

the Yaskawa MH24 robot controller (via an Human-Machine Interface (HMI)); (ii) the HRC safety mechanism (Section 5.3); (iii) the robot programming by demonstration framework (Section 5.4); (iv) the 6 Degrees of Freedom (DoF) point cloud alignment pipeline (Section 5.5). Figure 3 depicts a graphical representation of the adaptation of the logical system architecture of HORSE, as presented in [63], with the aforementioned components integrated into level 3.

5 Technology modules

In this section, the five technological pillars sustaining the collaborative coating cell concept will be detailed. These technological pillars were grouped in a functional architecture, depicted in Fig. 4, composed by four distinct and interoperable domains: (i) the HORSE framework layer; (ii) the agent layer; (iii) the application layer; and (iv) the hardware layer.

Section 5.1 will present the MPMS, that orchestrates the execution of actions defined as BPMN diagrams. Section 5.2 will present the employed HORSE Cyber-Physical Middleware, detailing the set of integration mechanisms developed to make the software modules developed in the experiment interoperable with the HORSE ecosystem. Section 5.3 will address the HRC safety mechanism that enables the collaboration and safe sharing of the workspace between the human operator and the industrial (non-collaborative) robot. Finally, Sections 5.4 and 5.5 detail the programming by demonstration framework and the 6 DoF point cloud alignment pipeline, respectively, that facilitate the collaborative coating operation.

Fig. 3 HORSE system logical software architecture, aggregation level 3, with FLEXCoating contributions (programming by demonstration; 6 degrees of freedom point cloud alignment pipeline; PILZ SafetyEYE) highlighted. Adapted from [63]

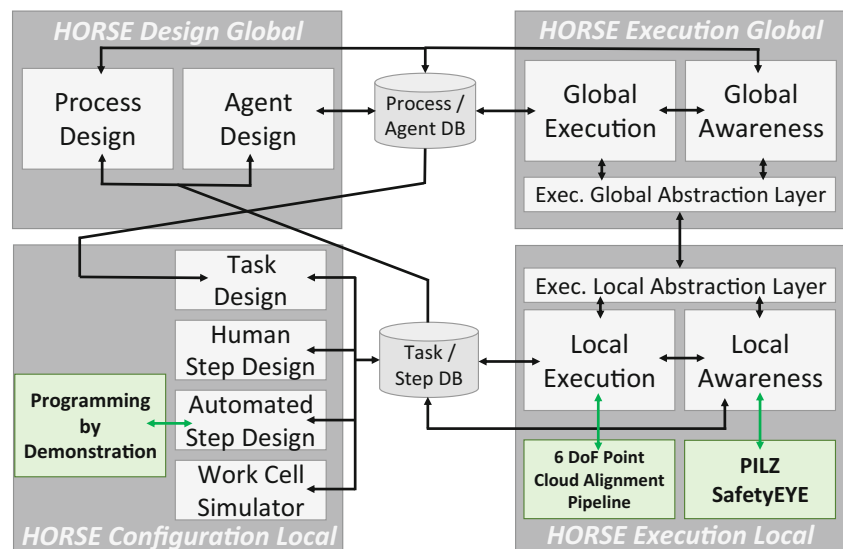
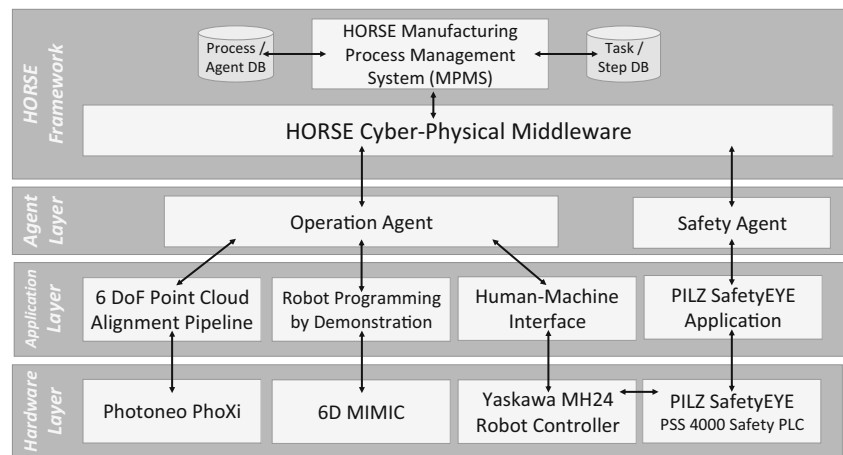


Fig. 4 Collaborative coating cell layer-based functional architecture, showcasing the integration of the proposed scientific contributions (application and agent layers) with the HORSE Framework and with the hardware layer



5.1 Manufacturing process management system

As previously addressed, one of the main scientific contributions of the HORSE project is the adaptation of BPMN models to support the execution of manufacturing tasks. Thus, one of the principal results of the HORSE research initiative is the development of the MPMS, a process management system which makes use of business process models, in particular the BPMN, for the orchestration of the manufacturing processes not only within a single work cell, but also across production lines. As detailed in [57], the MPMS module encompasses the totality of the HORSE Design Global domain of the architecture, including its process and agent design features. In addition, the MPMS also addresses the HORSE Global Execution domain of the architecture, making use of the Camunda technology [65], a powerful and open-source design tool and execution engine for BPMN workflows. Besides the orchestration responsibility, the MPMS also provides, through the Camunda Cockpit solution, a web-based dashboard that allows the monitoring of BPMN workflows, and administers interfaces for operators to input decisions that alter the execution flow, as well as output production information that allows operators to adapt their behaviour accordingly.

The MPMS component was used in three different areas: (i) the Camunda Modeler, a desktop application for modelling BPMN workflows, was used during the manufacturing process analysis step, detailed in Section 3, to create the BPMN models that describe the manufacturing process for the collaborative coating cell (see Figs. 1 and 2); (ii) the MPMS execution engine, based on the Camunda BPMN Workflow Engine, was utilized for the automated orchestration of services supported by the manufacturing processes' BPMN diagrams. For this, a set of adaptations were introduced to the MPMS process application layer to account for the use-case specific requirements, using the

provided Java Application Programming Interface (API). These adaptations ranged from the creation of application-specific services to the integration of end-user databases for the inventory of coating objects, the application PostgreSQL 9.5.14 relational databases to store robot trajectories imported from the 6D MIMIC system, and also to the development and integration of use-case specific HMIs; (iii) finally, the Camunda Cockpit module was used not only to monitor the execution flow but, more importantly, to allow operators to intuitively and easily interface with the system. The complete usage of the MPMS during an integration prototype can be seen in this video⁴.

5.2 HORSE Cyber-Physical Middleware

The HORSE framework besides enabling process modelling and process orchestration through the MPMS software, as addressed in the previous subsection, also provided the appropriate cyber-physical abstractions for promoting communication and interoperability amongst components. This abstraction layer, entitled the HORSE Cyber-Physical Middleware enabled the effective integration of the developed modules, that will be detailed in the following subsections, with HORSE-based components, such as the previously referred MPMS. The HORSE Cyber-Physical Middleware was developed on top of an OSGi middleware with integration components with relevant industrial ecosystems such as OPC-UA, the Robot Operating System (ROS), and the KUKA Sunrise system software [58].

In this work, the integration with the HORSE framework was enabled by employing the HORSE Cyber-Physical Middleware as a message broker to achieve communication between the different collaborative coating cell components and the MPMS. To achieve this interoperability, two middleware agents were implemented and are available as

⁴<https://youtu.be/wXmYIKQYmAY>

open-source contributions⁵. A general middleware agent was implemented as a Python class to handle the connection and communication through the HORSE Cyber-Physical Middleware, and two derived classes were implemented to act as two specific middleware agents, as depicted in Fig. 4: (i) a Safety Agent to handle the communication between the PILZ SafetyEYE system (Section 5.3) and the MPMS; and (ii) an Operation Agent to handle the communication between the 6 DoF point cloud alignment pipeline (Section 5.5), the 6D MIMIC system (Section 5.4), the Yaskawa MH24 robot controller, and the orchestration process running on the MPMS.

The Safety Agent began its behaviour by establishing a connection to a Modbus server running on the PSS 4000 safety Programmable Logic Controller (PLC). The Modbus server running on the PSS 4000 safety PLC provided a single coil that reflected the emergency state of the PILZ SafetyEYE system, which was monitored by the middleware agent, relaying this information to the MPMS when an alteration in the emergency state was detected. As will be clarified in Section 5.3, the direct safety I/O communication between the PILZ SafetyEYE system safety PLC and the Yaskawa MH24 robot controller were implemented using standard-compliant industrial safety procedures. Thus, it should be noted that the Safety Agent only provided the emergency state information to the MPMS for informative purposes, being relieved of any safety-related responsibilities.

The Operation Agent first connected to a rosbridge [66] server, that is, a WebSocket server serving as a communication interface with ROS applications, in this case, the 6 DoF point cloud alignment pipeline. It is also connected to socket servers acting as interfaces for the Yaskawa MH24 robot controller and to the 6D MIMIC system. The agent then waits for a message coming from the MPMS, notifying the start of a coating process. Upon receiving it, if the teaching phase of the process is executed, the agent requests the ROS application to store the reference point cloud of the positioning of the object during the programming by demonstration stage. Once the teaching is finalized, the robot trajectory was stored at a specific non-relational MPMS database, to be later retrieved during operation. When coating a given part, i.e. during the production phase, the Operation Agent is responsible for relaying the set of MPMS commands that would transfer the trajectory to the robot controller, trigger the 6 DoF point cloud alignment system to scan the environment for estimating the displacement of the object to be coated in relation to the teaching phase and relay to the Yaskawa controller the 6 DoF transformation for updating the robot trajectories.

⁵https://github.com/horse-flexcoating/horse_flexcoating_agents

5.3 Human-robot collaboration safety mechanism

The PILZ SafetyEYE sensor was used to provide the necessary safety mechanism to enable HRC. The sensor was employed to track the human operator position and the coating cell, thereby ensuring his/her safety while in a collaborative task. The PILZ SafetyEYE sensor records video with its three different cameras, which is then processed in its analysis unit. The latter is connected to the PSS 4000 safety PLC which acts as an interface with the rest of the system, allowing the monitoring of the emergency and warning states as well as the selection of the group of zones being monitored.

The setup procedure of the PILZ SafetyEYE equipment in the collaborative coating cell started by placing the setup and reference markers in the scene to be monitored, taking into consideration the positioning of the robot and the coating table, as seen in Fig. 5. The reference frame was chosen to be aligned with the lateral wall of the collaborative coating cell, to aid with the definition of the safety zones, in particular the one monitoring the side door, on the right side, as depicted in Fig. 5. In the same image, it is also possible to see the location of the reference markers, that would then be used during normal operation.

Figure 6 depicts the defined monitored zones: two detection zones and a reset zone were defined. The detection zone on the right side of the image is responsible for detecting intrusions coming from the lateral door of the cell, while the robot is in operation. This zone was configured to detect intrusions from 0.2 up to 0.55 m. Due to spatial restrictions of the cell, as it is close to the extremity of the monitorable area, it was impossible to extend the height of this zone. Nevertheless, this fairly restricted zone was deemed to be sufficient to detect lateral intrusions to the workspace.

The diagonal volume on the centre of Fig. 6 is the main detection zone in the collaborative coating cell. This zone is responsible for detecting an approximation by the coating operator (that would be operating in the space represented closer to the upper part of the image) to the coating robot (that is shown in the bottom part of the image). This zone is marked a few centimetres above the coating table (0.9 m), as to allow it to be freely moved without triggering the detection region. This zone extends to 1.9 m, which was considered to be more than sufficient to detect any intrusions by the operator.

Finally, the reset zone was defined on the left side of the image, at 1 m from the floor, and extending around 30 cm. This volume proved to be appropriate, during the demonstration of the collaborative coating cell, for the operator to signalize, by raising its left hand, that the robot could resume its movement after a danger zone was detected. A preliminary version of the collaborative coating

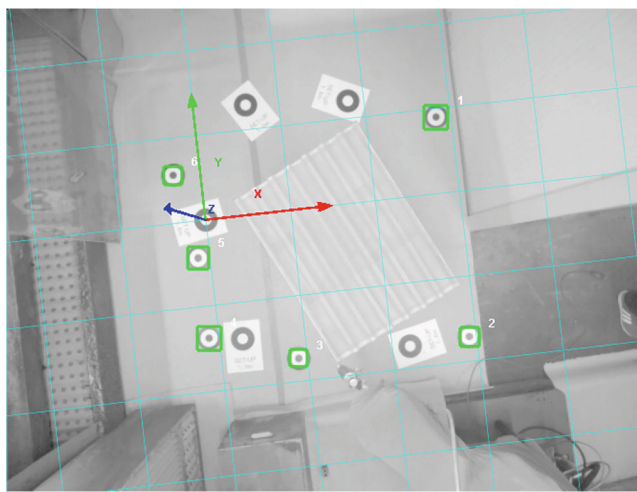


Fig. 5 PILZ SafetyEYE configuration stage: the reference markers are the smaller circular targets highlighted in green. The setup markers which are bigger, rectangular, and not highlighted, would be removed during nominal operation

cell had the operator signalizing the resume action by pressing a button located a few centimetres away from its operational area, which was considered inefficient as the operator needed to not only move to reach the button, but also to deposit the painting gun at an appropriate support.

The I/O connectivity between the PILZ SafetyEYE and the safety PLC was handled in such a way that the triggering of any of the two detection zones would trigger two (dual) safety Boolean variables to commute from True (safe to operate) to False (not safe to operate). Furthermore, the system was programmed in such a way that if any problematic condition was raised that directly impacted the safety assurance of the system (such as the impossibility to visualize the reference markers, which is needed to accurately detect intrusions to the zones), this safety Boolean variable would commute to False, thus signalizing an unsafe overall condition and directly commanding the robot to stop its movement. In addition, the reset signal was also mapped as a single Boolean variable, that would be triggered (i.e. changed to True) when the reset region was populated. This signal could only be active if the remainder detection zones would be clear, which signifies that the operator (or any other obstacle) had to be safely removed before the robot could resume its movement. These variables were mapped to a set of safety I/O signals accessible at the safety PLC that were then exported to the Yaskawa MH24 robot controller via safe dual-channel wiring.

5.4 Robot programming by demonstration

Close human-robot interaction for industrial manipulators is crucial to open new markets that cannot use fully automatic

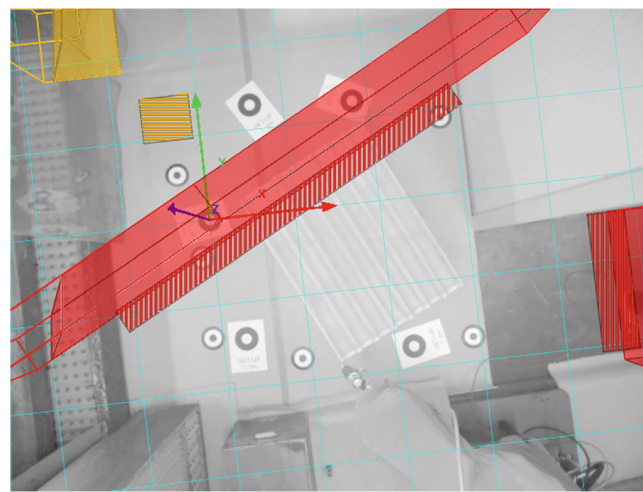


Fig. 6 PILZ SafetyEYE zone definition stage: two detection zones (represented in red) are defined in a diagonal volume between the operator working area and the rotating table, and in a volume closer to the coating cell door on the right side of the image; the reset zone (represented in yellow) is visible on the top left part of the image

systems due to, amongst others, the complexity of tasks and the cost of reprogramming new parts [67]. More in detail, the currently available commercial robot programming solutions, like teach pendants or kinetic teaching systems, still do not provide a way to precisely capture the human craftsmanship during the execution of complex operations, such as coating, painting, and others.

To answer to this requirement, some authors of this work and FLUPOL have worked together for several years on this topic, having created a high-level programming by demonstration framework, the 6D MIMIC solution [15], on the scope of the SIIARI project, which ultimately delivers the possibility of transferring human expertise to industrial robots.

The 6D MIMIC solution proposes a new approach for human motion tracking based on an innovative luminous 6D marker, that is coupled to the spray coating gun of the human operator, and together with a stereoscopic vision system, designed to track the 6D marker, allows the coating expert to teach by demonstration the coating operation to the industrial robot. This is accomplished by keeping the operators in his zone of comfort, and doing his everyday task. The industrial setup of the 6D MIMIC system is showcased in Fig. 7.

With this technology, the goal of allowing a shop floor operator to program an industrial manipulator with a complete abstraction of programming concepts has been achieved, as illustrated in the diagram depicted in Fig. 8.

In the scope of the coating cell conversion, the 6D MIMIC system was used to allow the human operator to teach the coating trajectory to the industrial robot in a completely transparent and intuitive manner. Furthermore,

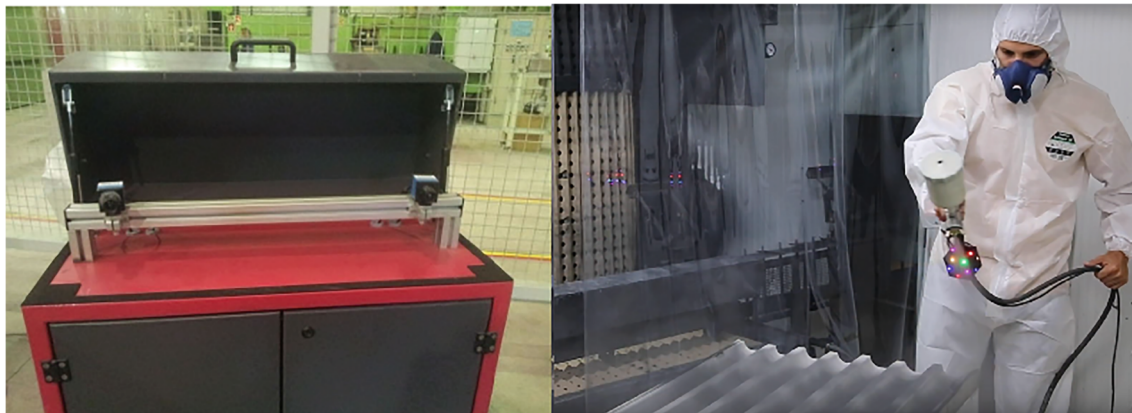


Fig. 7 Industrial setup of the 6D MIMIC system. It is constituted by a stereoscopic vision system mounted on an industrial cabinet (left figure) and the 6D marker attached to the operator's industrial spray coating gun (right figure) [15]

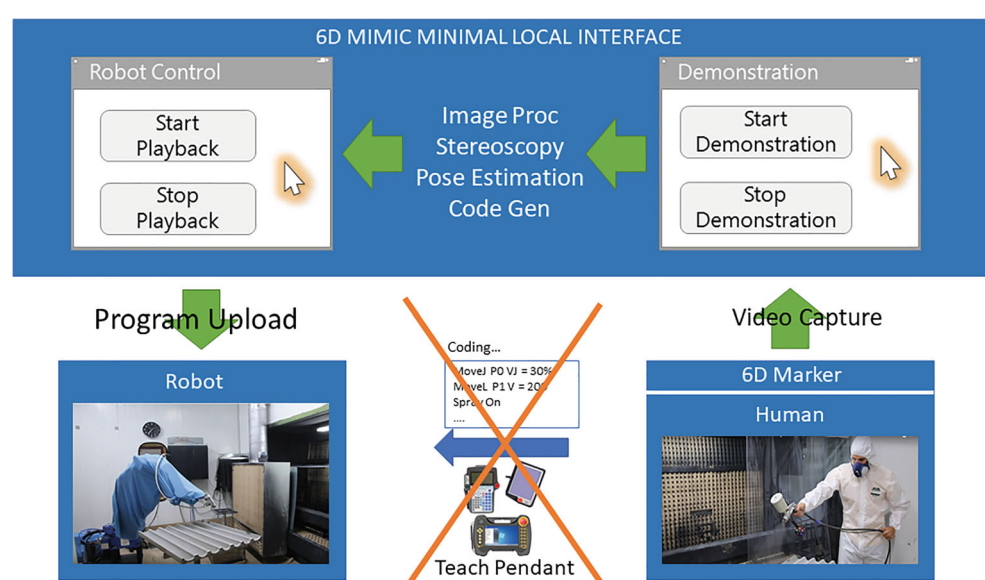
it was endowed with the proper industrial communication connectors, as detailed in Section 5.2 so to allow its integration with the HORSE Cyber-Physical Middleware.

Although the 6D MIMIC is in itself an asset for the programming process of the industrial robot, it requires the part to be coated to be positioned at the exact same 6 DoF pose during both the teaching by demonstration and robot production phases. This procedure, as can be easily extrapolated, has a significant impact on the setup time of the coating operation, further limiting the flexibility of the system. However, by coupling it with the 6 DoF point cloud alignment pipeline, described in Section 5.5, it becomes possible to drastically increase the tolerance of part positioning on the workstation, which was a significant contribution to the successful conversion of the coating cell to a collaborative one.

5.5 6 Degrees of freedom point cloud alignment pipeline

For avoiding the construction of fixtures for each specific part that needs to be coated, a 3D perception system was developed for estimating the translation and rotation offsets that were necessary to apply to the robot motions for properly coating the parts even when they were not placed in the 6 DoF pose in which the robot was taught by demonstration. Besides avoiding the cost of building fixtures, this capability improves the coating quality because it ensures that the relative motions between the robot coating tool and the part to be coated remain accurate. Moreover, by using the same hardware and work cell layout for coating all the parts, the robot could be

Fig. 8 The automatic generation of a robot program from the 6D tracking data. Each point is mapped into a robot movement instruction and the time stamp allows the definition of each segment speed [15]



quickly and remotely retasked for coating a wide range of products.

The 3D perception system was implemented as a ROS node (`pointcloud_registration`, available as an open-source contribution⁶) and several extensions were made to the Dynamic Robot Localization (DRL) system (described in [68]) for dealing with the collaborative coating cell use case.

Operation modes The 3D perception system was configured with two main modes of operation, which are shown in Fig. 9. The first mode was for setting up the system and dealt with the storage of point clouds that were associated with robot motions taught by demonstration. The second mode was used during production and was an extension of the first mode in which a point cloud alignment stage was added to the perception pipeline for computing the 6 DoF offset (translation and rotation) that was necessary to apply to the previously taught robot motions for taking into consideration the 6 DoF pose of the part to be painted in relation to the robot base. By performing the alignment in the same coordinate system as the robot trajectories (robot `base_link` frame), the 6 DoF correction transformation corresponded to the result of aligning the point cloud captured during teaching by demonstration with the point cloud acquired during production.

Object recognition algorithms were not necessary for performing the point cloud alignment because each set of robot trajectories taught by demonstration had associated the reference point cloud that was taken before the usage of the 6D MIMIC system. As such, when the operator used the HMI for specifying which set of trajectories he/she wanted the robot to perform, the 3D perception system was informed about the point cloud to use, while the Yaskawa robot controller received the associated trajectories.

Segmentation In the coating use case, the target objects were placed on top of a table whose position did not change significantly over time. As such, even with the uncertainty associated with the part placement on top of the table, the target object point cloud could still be easily segmented from the environment by defining a Region Of Interest (ROI) in a calibrated coordinate system followed by the selection of the 3D points that were within the ROI XYZ range thresholds.

The calibration of the ROI coordinate system was done by placing a ChArUco⁷ pattern on top of the table followed by the estimation of the camera 6 DoF pose in relation to the pattern origin. For tolerating displacements of the object on top of the table, the ROI was defined with its X and Y

⁶https://github.com/carlosmccosta/pointcloud_registration

⁷https://github.com/carlosmccosta/charuco_detector

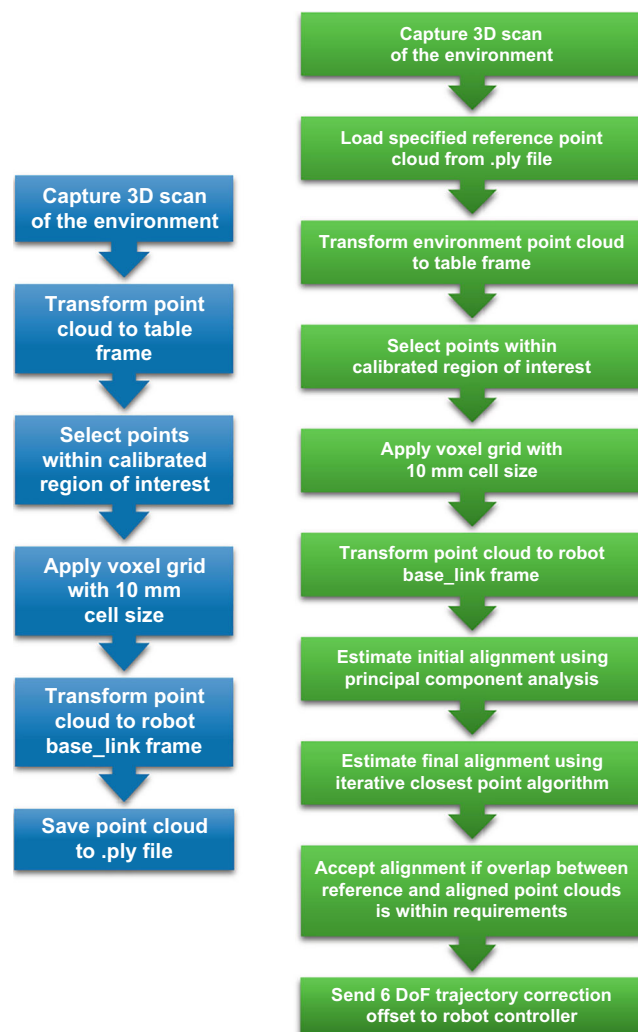


Fig. 9 Main processing stages of the 3D perception pipeline when storing reference point clouds (left) and aligning new sensor data for correcting the robot trajectories (right)

dimensions larger than the target object, while keeping a tight control over the Z dimensions for ensuring that the 3D points associated with the table would not be included in the segmented point cloud.

Filtering Given the runtime requirements of the coating work cell, the perception system was configured to process the least amount of data that allowed it to reach the desired accuracy as fast as possible. For controlling the level of detail extracted from the sensor data, a voxel grid algorithm with 10 mm cell size was used, which given the high resolution of the employed PhotoNeo XL 3D sensor (2064×1544), resulted in the reduction of the number of points within the ROI from around 30,000 to 8000. Considering that the runtime of the point cloud alignment algorithms is mostly linearly correlated with the number of

points that are provided, this filter allowed the alignment to run around 3 times faster.

The reason why there is only 30,000 points within the ROI is due to the fact that the Photoneo PhoXi XL 3D scanner had a high field of view and was placed close to the ceiling for avoiding damage from suspended particles coming from the robot or operator coating tools. The side effect was that the target objects occupied around 15% of the depth image. Nevertheless, the point density was still more than enough and was further reduced with the voxel grid, since a 10 mm Cartesian point density was empirically enough for the use case. On the other hand, having the sensor farther away provided higher flexibility to the operator, since the target object could be placed in a larger workspace.

Besides downsampling, several approaches were tested for reducing the sensor noise, such as the statistical outlier removal and radius outlier removal algorithms present in the Point Cloud Library (PCL). However, given the low noise generated by the 3D sensor, and their computation time of around 0.5 s, they were not deemed necessary and were not included in the perception pipeline.

Principal component analysis initial alignment The algorithms that are able to perform accurate point cloud registration [69] usually minimize the least-squares error between the reference and target point clouds by iteratively refining the point-to-point/point-to-plane correspondences or following gradients. The drawback is that they can fall into local minima and not reach the correct alignment. To tackle this problem, the reference and source point clouds must be roughly aligned with higher-level algorithms that do not work directly on the individual 3D points.

Within the initial alignment algorithms, several approaches are available in the state of the art. The most generic systems rely on the extraction of local 3D descriptors [70] that encode the 3D surface normals variation around 3D keypoints [71] followed by Random Sample Consensus (RANSAC) feature matching. Another approach computes a single global descriptor [72] for the entire object from a given point of view, which besides providing a rough 6 DoF pose by using kd-tree matching, it can also be used for object recognition. However, these systems are computationally intensive, and after testing the first method on the reference object sensor data, it was clear that they were not the best way to tackle this problem for this particular object, mainly because the reference objects had repeating geometry, resulting in a lot of similar keypoint descriptors being present in different places of the object, which in turn caused the matching process to succeed only when allowing the RANSAC algorithm to run for hundreds of iterations. Even though this approach implemented in the

DRL system was giving good results, it was taking several seconds to converge to good solutions.

After looking at alternative algorithms [73–75] and having in mind the use case object and the end-user requirements, a different and more efficient approach was implemented in DRL, in which the translation offsets between the reference and production point clouds were corrected using centroid displacement analysis and the rotation offsets were computed with principal component analysis (PCA).

The main drawbacks of PCA are related to the way it encodes the entire point cloud with a single 3×3 covariance matrix. Namely, PCS can only be used in objects that clearly have 3 different dimensions (as far from a cube as possible) and the object geometry must not change drastically when observed by the 3D sensor from the reference point cloud viewpoint and the production point cloud viewpoint. If these two requirements are not met, then another approach should be used for the initial alignment, such as feature matching, which can deal with a lot of object types but has the drawback of being computationally intensive. Unlike feature matching, that took around 4 s to compute, PCA only required 5 ms to perform the initial alignment for the reference object, while also empirically achieving less than 3 cm of translation error and less than 5 degrees of rotation error when compared with the final alignment. The PCA alignment error is due to the fact that the reference and production point clouds were retrieved from different viewpoints, which changes slightly what geometry is seen by the 3D sensor due to self-occlusions of the object, which in turn affect the centroid and covariance matrix computed by PCA.

On the other hand, the principal components present in the covariance matrix do not encode axes direction because they only capture the variance of the data. As such, the usage of PCA requires external information for knowing in which hemisphere the X+ and Z+ axes should be flipped (by rotating 180° around a perpendicular axis) for ensuring that the angle difference between the estimated PCA axes and the external reference axes is always below 180°. In DRL, these heuristics first align the X+ axis and then the Z+ axis, using as reference the robot base link coordinate system axes (as seen in Figs. 12 and 13).

The heuristics implemented on top of PCA for aligning its axes to an external reference frame allowed to make the perception system 100% repeatable when given the same data (unlike feature matching that is not repeatable, because it probabilistic converges to a solution using RANSAC). Moreover, these heuristics also solved the problem of the ambiguity that existed when estimating the 6 DoF pose of the reference object due to its symmetry axis along its longer length, which results in 2 perfectly valid poses from an alignment point of view. This ambiguity could negatively

affect the usage of the perception system if it was relying on feature matching, because it could select either one of these two 6 DoF poses. However, with the heuristics implemented on top of PCA, the perception system will always select the same 6 DoF pose out of the two possibilities, because only one of the candidates is on the hemisphere defined by the external X+ and Z+ axes.

Iterative closest point final alignment For accurately registering the reference point cloud with the production point cloud after the PCA initial alignment, the iterative closest point (ICP) algorithm [76] with the point-to-plane metric was used. By relying on the surface normals information, the least-squares minimization managed to empirically achieve less than 2 mm of translation error and less than 1° of rotation error. The accuracy of these experimental results was related to the level of detail that was given to ICP and the quality of the 3D point cloud. As such, increasing the resolution of the voxel grid or giving ICP all the segmented data would increase precision at the cost of processing time.

For tolerating large errors in the initial alignment stage while also ensuring robustness to sensor noise, the final alignment stage relied on the application of the ICP algorithm two times, but with different configurations. In the first ICP run, it was set with a maximum correspondence distance of 5 cm while on the second run the maximum correspondence distance was reduced to 1.5 cm for discarding any noise present in the sensor data.

In the end, a trade-off between precision and computation time was reached, by setting the voxel grid to 1 cm leaf size and limiting ICP to 500 iterations while giving ICP at most 1.8 s processing time for the first run and 0.7 s for the second run, resulting in a mean processing time of the entire perception system of around 2.5 s (for aligning the reference point cloud to the production point cloud, each with around 8000 points).

Registration validation For ensuring that the 3D perception pipeline correctly aligned the reference point cloud with the production point cloud, a postprocessing stage was added for computing the percentage of overlap between the two point clouds. A point in the production point cloud was considered as correctly aligned if there was a point in the reference point cloud at a distance of at most 2 cm (double of the voxel grid leaf size). Even though the perception pipeline achieved 100% overlap during our experimental evaluation, the alignment was only considered valid if the overlap was at least 88%. The reason why this threshold was not set to 100% is related to the fact that observing the reference object from different viewpoints may result in different surfaces to be seen or occluded from the 3D sensor point of view, and as such, the acceptable overlapping percentage must be lower than 100% for taking this into account.

6 Industrial demonstration and validation

The collaborative coating cell concept, fully integrated with the HORSE ecosystem, was validated under a real industrial environment, with real operators, and real production components at the end-user industrial facilities in Portugal. The final realization of the collaborative coating cell is depicted in Fig. 10. On the left side of the image, the Yaskawa MH24 robot is shown with a protective cover and a painting tool on its end-effector. The PILZ SafetyEYE and the Photoneo PhoXi 3D Scanner sensors can be seen at the top centre and top right side of the picture, respectively. In addition, an example part can be seen positioned on the top of the coating table, at roughly the centre of the image. The collaborative coating cell also features an extractor and oven, pictured at the left side of the figure, which are responsible for physically removing the over-spraying to the exterior of the cell, and help on the adherence of the applied coating product to the coated part, respectively. Outside of the coating cell, not pictured in Fig. 10, are also some other constituents of the system, namely the PILZ SafetyEYE processing unit and the corresponding safety PLC, the Yaskawa MH24 robot controller, and the computer running the MPMS and the HORSE Cyber-Physical Middleware, as described in Section 5.

The industrial demonstration and validation of the collaborative coating cell were conducted following a systematic strategy. On the one hand, during the design stage of the cell, the quality requirements applicable in the end-user production context were identified. These requirements were defined by the products standards and the quality criteria relevant in this industrial sector. On the other hand, the set of requirements were used to conduct an evaluation of the performance of the collaborative coating cell after deployment, which served a double purpose of attesting the industrial effectiveness of the proposed solution, and also comparing the collaborative solution with the traditional fully manual or fully automated coating operations, qualifying and quantifying, wherever possible, the overall productivity gains achieved.

For accomplishing this objective, and considering the SME's production scenario, a set of manufacturing performance metrics, or Key Performance Indicators (KPIs) were defined. In the interest of brevity, only the most scientific relevant KPIs will be discussed in this section.

Production quality In the design stage, production quality was defined by a direct comparison between the thickness of the coating applied in a collaborative way or a fully manual/fully automated fashion. Although coat thickness is an important measure to assess the quality of a coated component, it was later identified that it is more important that the applied coat is uniform and without missed spots in the object. As a result, the production quality KPI reflects

a visual qualitative evaluation, taking into consideration the uniform distribution of the coating material as well as its thickness. During the demonstration stage, it was verified by the end-user that the production quality of the collaborative coating cell was improved in up to 30%, according to the subject part, when in comparison with the fully manual/fully automated approach, as the human operator could correct mistakes produced by the robot collaboratively and efficiently.

Throughput increase The analysis of the current production of FLUPOL shows that up to 30% of the parts are handled manually, due to complexity and size. Due to the above-mentioned problems with training of skilled operators, FLUPOL's capacity for this type of product is exhausted, and therefore the use of the collaborative robotic cell, endowed with the five technological pillars

presented earlier, allowed to increase the overall throughput of FLUPOL in 15%. It should be noted that the increased throughput is achieved in complex parts, which means a significant increase in the competitiveness of the end-user.

Optimization of operator's usage This indicator represents the improvement to the effectiveness of the coating operator and its added value usage in the production process. In a fully manual coating scenario, the coating operator is completely responsible for applying the totality of the coat to every part. This results in inefficient utilization of the operator's best characteristics, as he/she spends a substantial amount of time in coating large surfaces applying repetitive movements that could be automated. The resulting collaborative coating cell allows operators to focus on where their effectiveness is more enhanced. In specific, by allowing operators to concentrate on operations that

Fig. 10 Final arrangement of the collaborative coating cell installed at the end-user industrial facilities



Fig. 11 FLEXCoating demonstration video⁸ snapshot showcasing an intrusion by the operator to a safety zone



cannot be effectively automated, there is an optimization of the operator's time allocation, estimated by the end-user company to be, on average, around 10% for the overall process. For complex or large parts, depending on their morphological characteristics, it is expected that the workload could be split in half between the robot and the operator, thus vastly improving the optimization of operators' time allocation.

Safety During nominal operation, the PILZ SafetyEYE system was responsible for ensuring the safety of the collaboration between the human operator and the coating robot. As it can be seen in Fig. 11 and also in a video⁸ which illustrates the complete FLEXCoating experiment industrial demonstration, the robot movement is safely halted when an intrusion is detected. For testing and assessing if the safety mechanism behaviour is according to the ISO 13849-1 [77], Performance Level (PL) d, 16 intrusions experiments were conducted in different arrangements for each detection zone. Considering a standard body-type invasion with 200 mm, the longest response time was calculated to be 275 ms, which was deemed to be compliant with the dimensions of the regions to avoid a collision between the robot and the operator given the maximum movement speed of the robot [31].

6 DoF point cloud alignment For testing the effectiveness, robustness, and time requirements of the 6 DoF point cloud alignment pipeline, several experiments were performed with reference objects placed at different positions and orientations on top of the table for both operation modes presented in Fig. 9. An example of the setup phase is

given in Fig. 12, which shows the reference point cloud generated by the 3D perception system (associated with a set of robot motions taught by demonstration using the 6D MIMIC system). On the top image of Fig. 12 it can be seen an overview of the work cell, in which it is shown the coordinate systems associated with the table frame, the robotic arm base_link frame and the PhotoNeo XL camera_link frame, along with the full point cloud that was generated by the 3D sensor.

In Fig. 13 is presented two results of the point cloud alignment pipeline (overlaid on top of the point clouds captured by the 3D sensor), in which the blue spheres display the reference point cloud, the orange spheres represent the initial alignment computed with PCA and the green spheres correspond to the final alignment achieved using the ICP algorithm. It can be observed that the usage of PCA for initial alignment followed by ICP for registration refinement is an approach that can effectively deal with large pose offsets of the target part during production (when compared with the teaching stage), while also achieving high accuracy point cloud alignment. After dozens of tests performed with the reference objects in different poses for evaluating its time requirements, the 3D perception pipeline required on average 2.5 s for computing the 6 DoF transformation necessary to update the robot trajectories (when using a Clevo N170RD laptop equipped with an Intel i7-6700HQ CPU and with 8 GB of DDR3 RAM).

For having a second layer of inspection of the results of the perception pipeline, the 6 DoF transformations estimated by the 3D perception system were represented on the top images of Fig. 13 as a new coordinate system named trajectory correction. It can be seen that the relative pose between the aligned reference object (green spheres) and the trajectory correction

⁸<https://youtu.be/3IZLhLpHyHE>

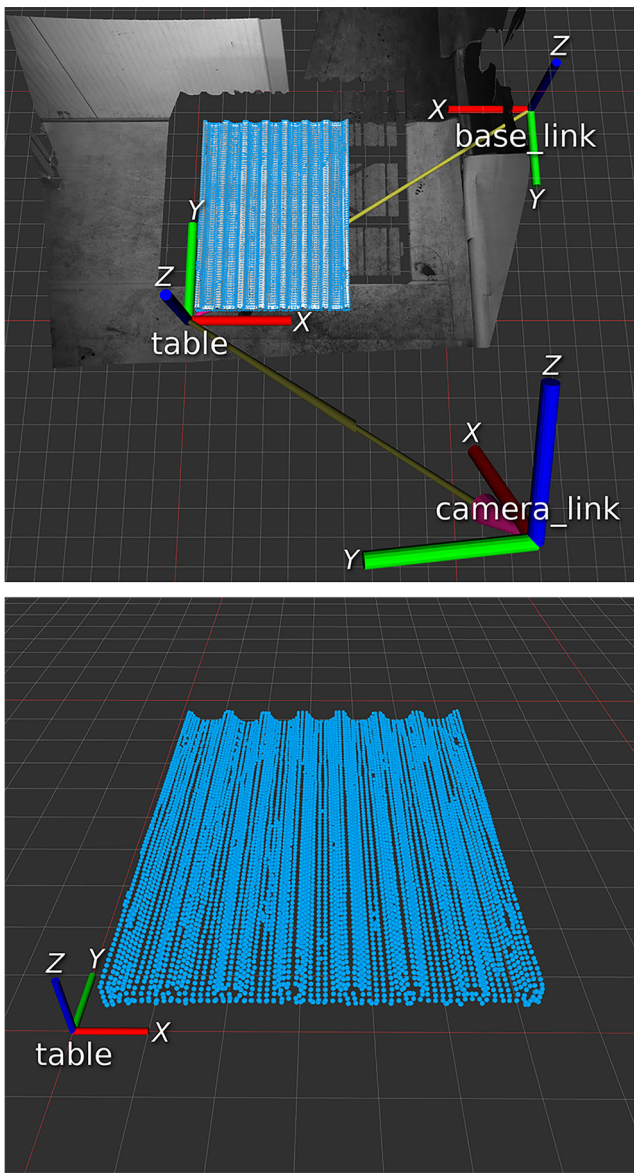


Fig. 12 Side (top) and closer (bottom) views of the generation of the reference point cloud (blue spheres) associated with the robot motions programmed by demonstration

frame during the production phase was practically the same as the relative pose between the reference object (blue spheres) and the robot base_link frame during the teaching phase.

Empirically, comparing the outline of the sensor data associated with the reference object with the aligned reference point cloud, it is possible to state that the perception pipeline seemed to have less than 2 mm of translation error and less than 1° of rotation error while achieving an overlap between the reference and production point clouds of 100%. A more precise evaluation would require an external ground truth system, which was not available at the time. But for the particular use case of

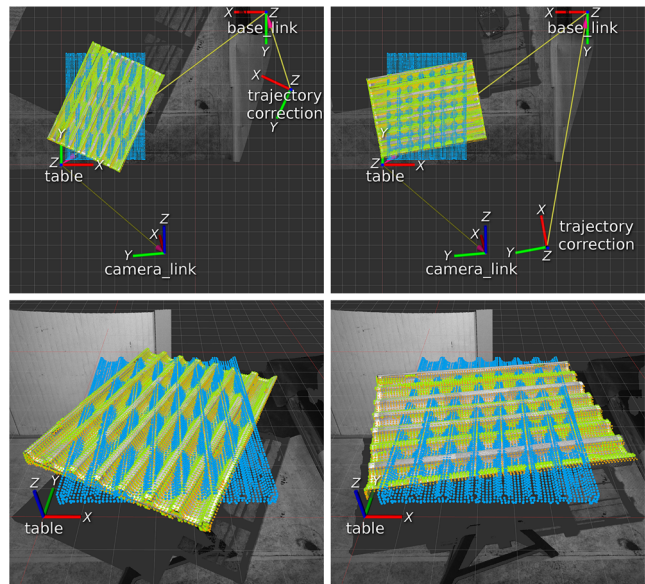


Fig. 13 Top-down (top) and closer (bottom) views of the results of the point cloud alignment (principal component analysis initial alignment shown with orange spheres and iterative closest point refinement displayed with green spheres) for correcting the reference object rotation offset of 25° (left) and 67° (right)

coating, up to 8 mm of deviation between the taught trajectory and the motions executed during production by the robot was deemed as acceptable by the end-user, which places the proposed work cell within the requirements imposed on the motion accuracy of the robot.

The 6D MIMIC system has on average an error of 3.8 mm and 1.7° of translation and rotation error, respectively, when tracking the marker attached to the painting tool. These tracking deviations are mainly due to the resolution of the stereo cameras and the overall calibration of the system. A more detailed analysis of the 6D MIMIC capabilities and performance can be found in [15].

On the other hand, the operator does not have millimetric accuracy when teaching the system by demonstration and he/she usually places the painting tool farther away from the target part for tolerating errors in the positioning of the painting tool, which also avoids over-spraying small regions (when holding the painting tool longer than the expected time).

As such, the robotic coating system as a whole was considered by the end-user as complying with its functional requirements in what concerns the accuracy of the robot motions. If in the future the accuracy requirement increases, the robotic system can be upgraded with a higher number or/and with higher resolutions industrial cameras for the 6D MIMIC system and more accurate 3D sensors for updating the robot trajectories during production.

7 Conclusion and future work

This paper demonstrated the adaptation of a fully automated robotic solution to a collaborative robotic cell for coating applications. The transformation was possible due to the development, integration, deployment, and industrial assessment of five technology modules. The MPMS and the HORSE Cyber-Physical Middleware allowed full interoperability with the HORSE ecosystem, enabling the orchestration of manufacturing tasks, and promoting the horizontal integration of the different hardware components composing the system, respectively. The integration of (i) the HRC safety mechanism, (ii) the robot programming by demonstration, and (iii) the 6 DoF point cloud alignment pipeline compose the main scientific contribution of this work. These modules enabled the industrial validation of the resulting collaborative robotic coating cell in a real production environment⁸, thus allowing improvements in production quality and efficiency.

As a concluding argument, it is possible to attest that this paper presents an approach for bringing a fully interoperable and collaborative robotic system to an industrial sector that is facing many business and production challenges as a result of the ongoing industrial revolution. The work presented in this paper made it possible for the end-user to rely on HRC to effectively increase productivity, quality, and market reach. Nevertheless, the system still faces natural scalability issues associated with hardware constraints. As an example, the dimensions and morphological characteristics of the objects to be coated are still majored by the field of view of the 6 DoF tracking sensor.

It is expected that some of the contributions presented in this paper can be applied to other SMEs facing similar issues in cross-sectorial industrial domains, thus extrapolating the impact that the presented technological advancement is having on the coating industrial sector to other potential beneficiaries.

The future work for this effort in bringing collaborative robotics to the coating sector will be ensured by the upcoming participation in the H2020 COVR project open-call [78]. With this new R&D effort, three objectives will be pursued: (i) utilize the specialized know-how and tools of the COVR initiative to assess, validate, and refine the safety features that would allow the industrialization of the collaborative coating cell concept; (ii) explore different safety technologies to achieve the desired collaborative behaviour, in an attempt to industrialize a more competitive solution from a production cost point of view; and (iii) contribute to enhancing the COVR protocols with the expertise acquired from applying the approach and tools to a collaborative robotic coating cell. Furthermore, ongoing efforts are being made to industrialize the collaborative coating cell concept, specifically by addressing the integration of the cell components with the end-user enterprise-level systems.

Funding The research leading to these results has received funding from the European Union's Horizon 2020 - The EU Framework Programme for Research and Innovation 2014–2020, under grant agreement no. 680734. This work has also been financed by National Funds through the Portuguese funding agency, FCT - Fundação para a Ciência e a Tecnologia within project UIDB/50014/2020.

Compliance with ethical standards

Conflict of interest The authors declare that they have no conflict of interest.

References

- Jazdi N (2014) Cyber physical systems in the context of industry 4.0. In: Automation, quality and testing, robotics, 2014, IEEE International Conference on. IEEE, pp 1–4. <https://doi.org/10.1109/AQTR.2014.6857843>
- Cohen Y, Faccio M, Pilati F, Yao X (2019) Design and management of digital manufacturing and assembly systems in the Industry 4.0 era. Int J Adv Manuf Technol 105(9):3565–3577. <https://doi.org/10.1007/s00170-019-04595-0>
- Rojas RA, Rauch E (2019) From a literature review to a conceptual framework of enablers for smart manufacturing control. Int J Adv Manuf Technol 104(1–4):517–533. <https://doi.org/10.1007/s00170-019-03854-4>
- Sethi P, Sarangi SR (2017) Internet of things: architectures, protocols, and applications. J Electric Comput Eng 2017. <https://doi.org/10.1155/2017/9324035>
- Li K, Zhou T, Liu Bh (2020) Internet-based intelligent and sustainable manufacturing: developments and challenges. Int J Adv Manuf TechnoL. <http://link.springer.com/10.1007/s00170-020-05445-0>
- Atzori L, Iera A, Morabito G (2010) The Internet of Things: a survey. Comput Netw 54(15):2787–2805. <https://doi.org/10.1016/j.comnet.2010.05.010>
- Kagermann H, Lukas WD, Wahlster W (2011) Industrie 4.0: Mit dem internet der dinge auf dem weg zur 4. industriellen revolution, VDI nachrichten, 13(11)
- Drath R, Horch A (2014) Industrie 4.0: hit or hype? [Industry Forum]. IEEE Ind Electron Mag 8(2):56–58. <https://doi.org/10.1109/MIE.2014.2312079>. <http://ieeexplore.ieee.org/document/6839101/>
- Hermann M, Pentek T, Otto B (2016) Design principles for industrie 4.0 scenarios. In: Proceedings of the Annual Hawaii International Conference on System Sciences 2016-March, pp 3928–3937. DOI:10.1109/HICSS.2016.488.. arXiv:[1011.1669v3](https://arxiv.org/abs/1011.1669v3)
- Keller M, Rosenberg M, Brettel M, Friederichsen N (2014) How virtualization, decentralization and network building change the manufacturing landscape: an Industry 4.0 perspective. Int J Mech Aerospace Ind Mechatron Manuf Eng 8(1):37–44
- Bocken NM, Short SW, Rana P, Evans S (2014) A literature and practice review to develop sustainable business model archetypes. J Clean Prod 65:42–56. <https://doi.org/10.1016/j.jclepro.2013.11.039>
- Frey CB, Osborne MA (2017) The future of employment: how susceptible are jobs to computerisation? Technol Forecast Soc Change 114:254–280. <https://doi.org/10.1016/j.techfore.2016.08.019>
- Sha L, Gopalakrishnan S, Liu X, Wang Q (2008) Cyber-physical systems: a new frontier. In: 2008 IEEE International Conference on Sensor Networks, Ubiquitous, and Trustworthy Computing

- (SUTC 2008), pp 1–9. <https://doi.org/10.1109/SUTC.2008.85>. <http://ieeexplore.ieee.org/document/4545732/>
14. Lee J, Bagheri B, Kao HA (2015) A cyber-physical systems architecture for Industry 4.0-based manufacturing systems. *Manuf Lett* 3:18–23. <https://doi.org/10.1016/j.mfglet.2014.12.001>
 15. Ferreira M, Costa P, Rocha L, Paulo Moreira A (2016) Stereo-based real-time 6-degrees of freedom work tool tracking for robot programing by demonstration. *Int J Adv Manuf Technol* 85(1–4):57–69. <https://doi.org/10.1007/s00170-014-6026-x>
 16. Ong S, Yew A, Thanigaiel N, Nee A (2020) Augmented reality-assisted robot programming system for industrial applications. *Robot Comput Integr Manuf* 101820:61. <https://doi.org/10.1016/j.rcim.2019.101820>
 17. Wojtynek M, Steil J, Wrede S (2019) Plug, plan and produce as enabler for easy workcell setup and collaborative robot programming in smart factories. *KI - Künstliche Intelligenz*. <https://doi.org/10.1007/s13218-019-00595-0>
 18. Krueger V, Rovida F, Grossmann B, Petrick R, Crosby M, Charzoule A, Garcia G, Behnke S, Toscano C, Veiga G (2019) Testing the vertical and cyber-physical integration of cognitive robots in manufacturing. *Robot Comput Integr Manuf* 57:213–229. <https://doi.org/10.1016/j.rcim.2018.11.011>
 19. Marvel JA (2017) Sensors for safe, collaborative robots in smart manufacturing. In: 2017 IEEE sensors, pp 1–3. <https://doi.org/10.1109/ICSENS.2017.8234264>
 20. Teke B, Lanz M, Kämäärinen J, Hietanen A (2018). In: 2018 14th IEEE/ASME International Conference on Mechatronic and Embedded Systems and Applications (MESA), pp 1–6. <https://doi.org/10.1109/MESA.2018.8449156>
 21. Samadikhoshkho Z, Zareinia K, Janabi-Sharifi F (2019) A brief review on robotic grippers classifications. In: 2019 IEEE Canadian Conference of Electrical and Computer Engineering (CCECE), pp 1–4. <https://doi.org/10.1109/CCECE.2019.8861780>
 22. Villani V, Pini F, Leali F, Secchi C (2018) Survey on human–robot collaboration in industrial settings: Safety, intuitive interfaces and applications. *Mechatronics* 55:248–266. <https://doi.org/10.1016/j.mechatronics.2018.02.009>
 23. Gervasi R, Mastrogiacomo L, Franceschini F (2020) A conceptual framework to evaluate human–robot collaboration. *Int J Adv Manuf* 108(3):841–865. <https://doi.org/10.1007/s00170-020-05363-1>
 24. Eimontaite I, Gwilt I, Cameron D, Aitken JM, Rolph J, Mokaram S, Law J (2019) Language-free graphical signage improves human performance and reduces anxiety when working collaboratively with robots. *Int J Adv Manuf* 100(1):55–73. <https://doi.org/10.1007/s00170-018-2625-2>
 25. Pérez L, Rodríguez-Jiménez S, Rodríguez N, Usamentiaga R, García D, Wang L (2020) Symbiotic human–robot collaborative approach for increased productivity and enhanced safety in the aerospace manufacturing industry. *Int J Adv Manuf* 106(3):851–863. <https://doi.org/10.1007/s00170-019-04638-6>
 26. Matúsová M, Bucányová M, Hrusková E (2019) The future of industry with collaborative robots. *MATEC Web Conf* 299:02008. <https://doi.org/10.1051/matecconf/201929902008>
 27. Technical Committee: ISO/TC 299 Robotics (2011a) ISO 10218-1:2011, Robots and robotic devices — Safety requirements for industrial robots— Part 1: Robots. Tech. rep., International Organization for Standardization
 28. Technical Committee: ISO/TC 299 Robotics (2011b) ISO 10218-2:2011, Robots and robotic devices — Safety requirements for industrial robots— Part 2: Robot systems and integration. Tech. rep., International Organization for Standardization
 29. Technical Committee: ISO/TC 299 Robotics (2016) ISO/TS 15066:2016, Robots and robotic devices — Collaborative robots. Tech. rep., International Organization for Standardization
 30. Villani V, Pini F, Leali F, Secchi C (2018) Survey on human–robot collaboration in industrial settings: safety, intuitive interfaces and applications. *Mechatronics* 55(June 2017):248–266. <https://doi.org/10.1016/j.mechatronics.2018.02.009>
 31. De Santis A, Siciliano B, De Luca A, Bicchi A (2008) An atlas of physical human–robot interaction. *Mech Mach Theory* 43(3):253–270. <https://doi.org/10.1016/j.mechmachtheory.2007.03.003>
 32. Pilz, Ria and Robotic Industries Association and others (2008) The first safe camera system safetyeye opens up new horizons for safety & security
 33. Magrini E, Ferraguti F, Ronga AJ, Pini F, Luca AD, Leali F (2020) Human–robot coexistence and interaction in open industrial cells. *Robot Comput Integr Manuf* 101846:61. <https://doi.org/10.1016/j.rcim.2019.101846>
 34. Tsarouchi P, Matthaiakis AS, Makris S, Chryssolouris G (2017) On a human–robot collaboration in an assembly cell. *Int J Comput Integr Manuf* 30(6):580–589. <https://doi.org/10.1080/0951192X.2016.1187297>
 35. Neto P, Simão M, Mendes N, Safeea M (2019) Gesture-based human–robot interaction for human assistance in manufacturing. *Int J Adv Manuf* 101(1):119–135. <https://doi.org/10.1007/s00170-018-2788-x>
 36. Tavares P, Costa C, Rocha L, Malaca P, Costa P, Moreira A, Sousa A, Veiga G (2019) Collaborative welding system using BIM for robotic reprogramming and spatial augmented reality. *Autom Constr* 106:102825. <https://doi.org/10.1016/j.autcon.2019.04.020>
 37. Krueger V, Rovida F, Grossmann B, Petrick R, Crosby M, Charzoule A, Garcia GM, Behnke S, Toscano C, Veiga G (2019) Testing the vertical and cyber-physical integration of cognitive robots in manufacturing. *Robot Comput Integr Manuf* 57:213–229. <https://doi.org/10.1016/j.rcim.2018.11.011>
 38. Lenz C, Nair S, Rickert M, Knoll A, Rosel W, Gast J, Bannat A, Wallhoff F (2008) Joint-action for humans and industrial robots for assembly tasks. In: RO-MAN 2008 - The 17th IEEE International Symposium on Robot and Human Interactive Communication, pp 130–135. <https://doi.org/10.1109/ROMAN.2008.4600655>
 39. Fast-Berglund Å, Romero D (2019) Strategies for implementing collaborative robot applications for the operator 4.0. In: Production Management for the Factory of the Future. APMS 2019. IFIP Advances in Information and Communication Technology, IFIP International Federation for Information Processing, pp 682–689. https://doi.org/10.1007/978-3-030-30000-5_83
 40. Cherubini A, Passama R, Navarro B, Sorour M, Khelloufi A, Mazhar O, Tarbouriech S, Zhu J, Tempier O, Crosnier A, Fraisse P, Ramdani S (2019) A collaborative robot for the factory of the future: Bazar. *Int J Adv Manuf* 105(9):3643–3659. <https://doi.org/10.1007/s00170-019-03806-y>
 41. Johannsmeier L, Haddadin S (2017) A hierarchical human–robot interaction-planning framework for task allocation in collaborative industrial assembly processes. *IEEE Robot Autom Lett* 2(1):41–48. <https://doi.org/10.1109/LRA.2016.2535907>
 42. Makrini IE, Merckaert K, Lefebvre D, Vanderborght B (2017) Design of a collaborative architecture for human–robot assembly tasks. In: 2017 IEEE/RSJ International Conference on Intelligent Robots and Systems (IROS), pp 1624–1629. <https://doi.org/10.1109/IROS.2017.8205971>
 43. Martínez S, Carvajal A, Loza D, Ibarra A, Segura L (2017) Collaborative two-arm robotic torso for the development of an assembly process
 44. Zeng F, Xiao JY, Liu H (2019) Force/torque sensorless compliant control strategy for assembly tasks using a 6-DoF collaborative robot. *IEEE Access* 7:108795–108805. <https://doi.org/10.1109/ACCESS.2019.2931515>

45. Sadrfaridpour B, Wang Y (2018) Collaborative assembly in hybrid manufacturing cells: an integrated framework for human–robot interaction. *IEEE Trans Autom Sci Eng* 15(3):1178–1192. <https://doi.org/10.1109/TASE.2017.2748386>
46. Cherubini A, Passama R, Crosnier A, Lasnier A, Fraisse P (2016) Collaborative manufacturing with physical human–robot interaction. *Robot Comput Integr Manuf* 40:1–13. <https://doi.org/10.1016/j.rcim.2015.12.007>
47. Accorsi R, Tufano A, Gallo A, Gajhlizia F, Cocchi G, Ronzoni M, Abbate A, Manzini R (2019) An application of collaborative robots in a food production facility, vol 38, pp 341–348, <https://doi.org/10.1016/j.promfg.2020.01.044>. 29th International Conference on Flexible Automation and Intelligent Manufacturing (FAIM 2019), June 24–28, 2019, Limerick, Ireland, Beyond Industry 4.0: Industrial Advances, Engineering Education and Intelligent Manufacturing
48. Siciliano B, Khatib O (2007) Springer handbook of robotics. Springer, Berlin
49. Chen H, Xi N (2008) Automated tool trajectory planning of industrial robots for painting composite surfaces. *Int J Adv Manuf* 35(7–8):680–696
50. Wang Z, Fan J, Jing F, Liu Z, Tan M (2019) A pose estimation system based on deep neural network and ICP registration for robotic spray painting application. *Int J Adv Manuf* 104(1):285–299. <https://doi.org/10.1007/s00170-019-03901-0>
51. Asadi E, Li B, Chen I (2018) Pictobot: a cooperative painting robot for interior finishing of industrial developments. *IEEE Robot Autom Mag* 25(2):82–94. <https://doi.org/10.1109/MRA.2018.2816972>
52. Object Management Group (2011) Business process model and notation 2.0 specification. <https://www.omg.org/spec/BusinessProcessModelNotation/2.0/>
53. Silver B (2011) Bpmn method and style, with bpmn implementer's guide: a structured approach for business process modeling. sl: Cody
54. List B, Korherr B (2006) An evaluation of conceptual business process modelling languages. In: Proceedings of the 2006 ACM Symposium on Applied Computing, pp 1532–1539. <https://doi.org/10.1145/1141277.1141633>
55. Dumas M, La Rosa M, Mendling J, Reijers HA et al (2013) Fundamentals of business process management, vol 1. Springer, Berlin. <https://doi.org/10.1007/978-3-662-56509-4>
56. Erasmus J, Vanderfeesten I, Tragano K, Jie-A-Looi X, Kleingeld A, Grefen P (2018) A method to enable ability-based human resource allocation in business process management systems. In: IFIP Working Conference on the Practice of Enterprise Modeling, pp publisher=Springer, 37–52. https://doi.org/10.1007/978-3-030-02302-7_3
57. Vanderfeesten I, Erasmus J, Tragano K, Bouklis P, Garbi A, Boultadakis G, Dijkman R, Grefen P (2019) Developing process execution support for high-tech manufacturing processes. In: Empirical studies on the development of executable business processes. Springer, pp 113–142. https://doi.org/10.1007/978-3-030-17666-2_6
58. Grefen P, Vanderfeesten I, Boultadakis G (2018) Developing a cyber-physical system for hybrid manufacturing in an internet-of-things context. In: Protocols and applications for the industrial internet of things. IGI Global, pp 35–63. <https://doi.org/10.4018/978-1-5225-3805-9.ch002>
59. Kruchten PB (1995) The 4+1 view model of architecture. *IEEE Softw* 12(6):42–50. <https://doi.org/10.1109/52.469759>
60. Grefen P, Eshuis R, Mehandjiev N, Kouvas G, Weichhart G (2016) Business information system architecture fall 2016 edition. Eindhoven University of Technology, Eindhoven
61. Erasmus J, Vanderfeesten I, Tragano K, Grefen P (2018) The case for unified process management in smart manufacturing. In: 2018 IEEE 22nd International Enterprise Distributed Object Computing Conference (EDOC). IEEE, pp 218–227. <https://doi.org/10.1109/EDOC.2018.00035>
62. Grefen P, Vanderfeesten I, Boultadakis G (2015) D2. 2a-complete system design-public version, Tech. rep., Eindhoven University of Technology
63. Erasmus J, Grefen P, Vanderfeesten I, Tragano K (2018) Smart hybrid manufacturing control using cloud computing and the internet-of-things. *Machines* 6(4):62. <https://doi.org/10.3390/machines6040062>
64. International Electrotechnical Commission (2003) International electrotechnical commission 62264-1 enterprise-control system integration—part 1: models and terminology. IEC, Genf
65. Camunda Services GmbH (2020) Camunda: Process Automation Reinvented for the Digital Enterprise. <https://camunda.com/>
66. Crick C, Jay G, Osentoski S, Pitzer B, Jenkins OC (2017) Rosbridge: Ros for non-ros users. In: Robotics research. Springer, pp 493–504. https://doi.org/10.1007/978-3-319-29363-9_28
67. Argall BD, Chernova S, Veloso M, Browning B (2009) A survey of robot learning from demonstration. *Rob Auton Syst* 57(5):469–483. <https://doi.org/10.1016/j.robot.2008.10.024>
68. Costa CM, Sobreira HM, Sousa AJ, Veiga GM (2016) Robust 3/6 dof self-localization system with selective map update for mobile robot platforms. *Robot Auton Syst* 76:113–140. <https://doi.org/10.1016/j.robot.2015.09.030>
69. Sahin C, Garcia-Hernando G, Sock J, Kim TK (2020) A review on object pose recovery: from 3d bounding box detectors to full 6d pose estimators. *Image Vis Comput* 103898:96. <https://doi.org/10.1016/j.imavis.2020.103898>
70. Rusu RB, Blodow N, Beetz M (2009) Fast point feature histograms (fpfh) for 3d registration. In: 2009 IEEE International Conference on Robotics and Automation, pp 3212–3217
71. Filipe S, Alexandre LA (2014) A comparative evaluation of 3d keypoint detectors in a rgb-d object dataset. In: 2014 International conference on computer vision theory and applications (VISAPP), vol 1, pp 476–483
72. Rusu RB, Bradski G, Thibaux R, Hsu J (2010) Fast 3d recognition and pose using the viewpoint feature histogram. In: 2010 IEEE/RSJ International Conference on Intelligent Robots and Systems, pp 2155–2162
73. Bellekens B, Spruyt V, Berkvens R, Penne R, Weyn M (2015) A benchmark survey of rigid 3d point cloud registration algorithms. *Int J Adv Intell Syst* 1
74. Yuan C, Yu X, Luo Z (2016) 3d point cloud matching based on principal component analysis and iterative closest point algorithm. In: International Conference on Audio, Language and Image Processing (ICALIP), pp 404–408
75. Li F, Stoddart D, Hitchens C (2017) Method to automatically register scattered point clouds based on principal pose estimation. *Opt Eng* 56(4):1–10. <https://doi.org/10.1117/1.OE.56.4.044107>
76. Besl PJ, McKay ND (1992) A method for registration of 3-d shapes. *IEEE Trans Pattern Anal Mach Intell* 14(2):239–256
77. Hedberg J, Söderberg A, Tegehall J (2011) How to design safe machine control systems: a guideline to en iso 13849-1
78. Bessler J, Schaake L, Bidard C, Buirke JH, Lassen AE, Nielsen K, Saenz J, Vicentini F (2018) Covr—towards simplified evaluation and validation of collaborative robotics applications across a wide range of domains based on robot safety skills. In: International Symposium on Wearable Robotics. Springer, pp 123–126. https://doi.org/10.1007/978-3-030-01887-0_24